Intelligent Damage Classification and Estimation in Power Distribution Poles Using Unmanned Aerial Vehicles and Convolutional Neural Networks

Mohammad Mehdi Hosseini, *Student Member, IEEE*, Amarachi Umunnakwe, *Student Member, IEEE*, Masood Parvania, *Senior Member, IEEE*, and Tolga Tasdizen, *Senior Member, IEEE*

***Abstract*—Damage estimation is part of daily operation of power utilities, often requiring a manual process of crew deployment and damage report to quantify and locate damages. Advancement in unmanned aerial vehicles (UAVs) as well as real-time communication and learning technologies could be harnessed towards efficient and accurate automation of this process. This paper develops a model to automate the process of estimating and localizing damages in power distribution poles, which utilizes the images taken by UAVs transferred in real-time to an intelligent damage classification and estimation (IDCE) unit. The IDCE unit integrates four convolutional neural networks to learn the states of poles from images, extract the image characteristics, and train an automated intelligent tool to replace manual fault location and damage estimation. The proposed model first determines the type of pole damages, including falling and burning, and then estimates the percentage of damage in each type. The IDCE unit also localizes damages in the poles by locating possible burning or arcing parts. A data set of 1615 images is utilized to train, validate and test the proposed model, which demonstrates high accuracy of the model in classifying and estimating damages in distribution poles.**

***Index Terms*—Deep neural network, damage classification and estimation, unmanned aerial vehicles, resilience.**

I. Introduction

MAJOR power outages affect millions of customers each year, including various businesses and critical infrastructure, costing them tens of billions of dollars. A large portion of long-time power outages results from external events affecting power systems, including hurricanes, ice storms, and other severe weather incidents [1], [2]. From over nine hundred major power outages in 2003-2012 in United States, in which more than 50,000 customers were affected, 726 outages were due to weather-related events [3]. Timely inspection and documenting problems and failures on grid equipment following an external event, as well as timely damage estimation and crew dispatch management are major contributors to reduce outage duration [4]. There are typically two sources of information available for utilities for inspecting power systems and damage estimation, namely power system data acquisition systems (such as communicating faulted circuit indicators), and visual inspection. Fault detection and sensory equipment are helpful to detect and locate electrical faults such as short circuit and high impedance faults, equipment failures, or transient harmonic sources. They can also detect existence of fire, smoke, or high temperature using various sensors throughout the grid. However, sensors working based on measuring fault current/voltage cannot detect passive physical damages and the extent of damages in the equipment.

Visual inspection is a routine procedure in the monitoring of power equipment, as well as an important step for repair and replacement process following disasters. Various methods have been utilized by utility companies for visual inspection, including foot patrols, helicopter assisted inspection, climbing robots, and deploying unmanned aerial vehicles (UAVs) along the power lines [5], [6]. More advanced inspection methods include synthetic aperture radar (SAR) imaging, satellite imaging, and land-based mobile mapping [7]. These complicated, and more expensive, methods are usually used for tasks beyond inspection, such as vegetation monitoring or conductor mapping. Utilization of UAVs for power system inspection has gained more attraction in recent years, as they come with lower cost, higher speed, and safer operation compared to the alternatives. Furthermore, UAVs – unlike helicopters – can fly close enough to power lines to provide detailed pictures, and yet – unlike climbing robots – be distant enough to capture the whole utility pole in one image. In 2015, Commonwealth Edison was the first utility in U.S. that received permission from the Federal Aviation Authority (FAA) to fly UAVs over its power grid [8]; since then almost all utilities started to use them to some extent. Utilizing UAVs for power line inspection does not come without a challenge, as they need to automatically navigate along the power system and to not wander off. UAVs also need to have navigation and detection capabilities, in order to take targeted images from power equipment. As for navigation, different methods have been utilized, which include GPS way points-based tracking, pole detection, and power line detection [9], [10].

Various object detection models based on deep neural networks are utilized for pole detection, which include Faster R-CNN [11], YOLO [12], and SSD [13]. In addition, state-of-art classifiers based on neural networks such as VGG-16 [14], ResNet [15], and Inception-v4 [16] can also classify pole images with high accuracy. "Pole" is one of many defined classes in ImageNet database [17], which most pre-trained networks are trained with, and that makes the pole-detection task rather easier. In [18], [19], images taken by

This work was supported by the Office of Naval Research under Grant N000141812395. M. M. Hosseini, A. Umunnakwe, M. Parvania and T. Tasdizen are with the Department of Electrical and Computer Engineering, the University of Utah, Salt Lake City, UT 84112 USA (e-mails: mehdi.hosseini@utah.edu, amarachi.t.umunnakwe@utah.edu, masood.parvania@utah.edu, tolga@sci.utah.edu).

This article has been accepted for publication in a future issue of this journal, but has not been fully edited. Content may change prior to final publication. Citation information: DOI 10.1109/TSG.2020.2970156, IEEE Transactions on Smart Grid

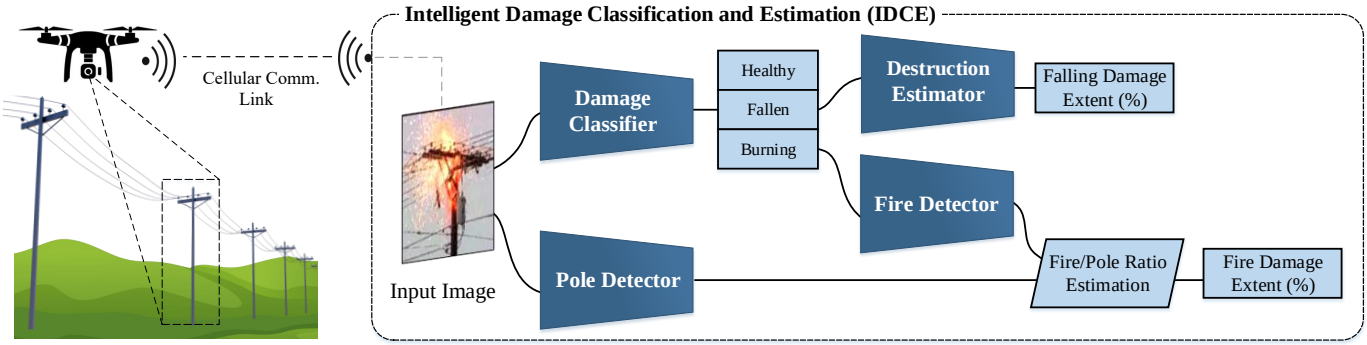

Fig. 1. Architecture of Intelligent Damage Classification and Estimation Unit

UAVs are used to train a fast R-CNN and YOLO models, respectively, in order to detect transmission towers and use that data in applications such as tree barrier modeling. Other techniques such as segmentation and track-and-detect methods have been also investigated in pole detection [20]. Power line detection, on the other hand, has proven more challenging than pole detection, as detecting thin wires over different backgrounds can be quite difficult. As such, various clustering and classifications combined with knowledge-based techniques have been employed for power line detection in [21]–[23].

Optical aerial images taken from power lines are also used for tasks other than the mere inspection of lines. In some research, the images from transmission and distribution lines, taken from UAVs or installed video cameras on poles and towers, are proposed to be used to detect icing condition of power lines [24], [25]. Vegetation encroachment monitoring is another application that employs optical images [26]. However, less attention has been given to the potential use of UAV imaging in disaster monitoring. With the advance of image classification and object detection, a proper damage detection and classification framework can significantly speed up the recovery process in widely-damaged power systems.

This paper develops a novel intelligent damage classification and estimation (IDCE) unit that is composed of four convolutional neural networks (CNNs) to identify the states and failure types of power line poles, and estimate the extent of the damage they sustained. The IDCE unit, shown in Fig. 1, receives images taken by UAVs that fly along the distribution feeders to take images of the power line poles. The large number of UAV images are first pre-processed and then utilized to train the CNNs in IDCE. The first CNN, called Damage Classifier, classifies input images into healthy, fallen and burning poles. Second CNN, called Destruction Estimator, is trained to estimate the damage extent in fallen poles as detected by the first CNN. For burning and arcing poles, two regression-based CNNs, namely Fire Detector and Pole Detector, localize the fire/arc over a pole and estimate the damage extent of fire/arc. The proposed IDCE unit conduct damage detection and estimation in real time, which speeds up disaster management and reduces required time and resources for distribution system inspection.

The rest of this paper is organized as follows. The architecture of IDCE unit along with the structure of CNNs and the training methods are presented in Section II. Image collection and pre-processing methods are described in Section III. The results of training, validating and testing the proposed ICDE unit using 1615 pole images are presented in Section IV, and conclusions are presented in Section V.

II. Damage Classification and Estimation Using Deep Convolutional Neural Networks

In the proposed framework in Fig. 1, the UAVs fly over distribution lines after a disaster (e.g., hurricane) and send images of distribution poles, along with their location, to a control center using cellular communication link. The cellular communication infrastructure is typically more resilient than power distribution systems and can be utilized after the disaster, as usually there exist more than one cellular service provider and there is a chance that at least one of them can survive the disaster (e.g., the case of AT&T survival in Panama City after Hurricane Michael while other operators were out [27]). UAVs may have access to multiple carriers as backup communication in such cases. In addition, cellular service providers can deploy portable satellite communication devices to areas cut from the service after a disaster. Even if cellular service is completely out in one location, the UAV can transmit its data once it flies into an area with service coverage.

The images captured by UAVs from power line poles could be taken from different angles, at different scales, with different resolutions, with various background objects, and at different times of the day. Therefore, the four CNNs in the proposed IDCE unit must be trained with voluminous images taken in different conditions. The IDCE unit includes a classification network to classify damage types, a regression network for damage estimation of fallen poles, and two regression networks for damage estimation due to fire and arc. Details of structures, training methods, loss functions, and scoring criteria used in the CNNs are presented next.

A. Structure of Convolutional Neural Networks

Convolutional neural network (CNN) is a variation of neural networks, consisting of input, output and hidden layers, which due to its special characteristics is mostly used for image classification and object detection applications. The CNNs make the explicit assumption that the input data are images, which allows detecting their spatial properties. That makes the implementation of forward function more efficient and

This article has been accepted for publication in a future issue of this journal, but has not been fully edited. Content may change prior to final publication. Citation information: DOI 10.1109/TSG.2020.2970156, IEEE Transactions on Smart Grid

significantly reduce the number of parameters in the network. CNNs utilize the local dot product to extract local features. For that, a rectangular $M \times M$ filter moves over a $N_1 \times N_2$ layer ($M < N_1, M < N_2$) and in each position, the dot product of the filter and the area of the layer overlapped by the filter provide a new value for the next layer. The filter parameters, i.e., w_{mn} $(m, n \in M)$, are optimized using back propagation method, which finds the gradient descent of the error or loss function over all hidden layers. Each 2-D layer along with its filters and activation function is a neuron that completes the following transformation over all its components:

$$Y_{jk}^{l} = f(\sum_{m=0}^{M-1}\sum_{n=0}^{M-1} w_{mn}^{(l)} X_{(j+m)(k+n)}^{(l)}), \tag{1}$$

where X and Y are input and output of hidden layer l, and f is the non-linear activation function. More number of filters may exist in one layer, resulting in a multi-channel output. In addition, pooling layers, added after or between convolutional layers, reduce the spatial size of the input and risk of overfitting. Max-pooling layers, used in this paper, take a $P \times P$ region of the input and generate a single value, which is the maximum of the input region. If CNN is expected to have a vector as output, it may end with a fully connected layer with the same size as the output vector. In classifier networks the fully connected layer is followed by a Softmax layer to generate a one-hot encoded vector, that is, a binary vector in which only one of the elements, corresponding to a specific class, is 1 and other elements are zero.

The loss function provides a measure indicating how the values predicted by the neural network match the actual values. The form of the loss function is determined based on the type of input and output data. For regression-based networks with a numerical output, the least square function may be used as loss function, while classification networks usually use cross entropy function to calculate the loss. Generally, we may define the loss function for a neural network as:

$$L(w, b) = \frac{1}{N^S}\sum_{i=1}^{N^S} \sigma(Y_i - \hat{Y}_i) \tag{2}$$

where σ is an arbitrary measure of difference, N^S is the total number of samples, and Y and $\hat{Y}$ are actual and predicted output values, respectively. In each training iteration t values of convolutional filters, also called weights, are updated by back propagation of the gradient of the loss function over all hidden layers in between:

$$w_l^{(t+1)} = w_l^{(t)} - \eta \frac{\partial L}{\partial Y_{N^l}^{(t)}} \cdot \frac{\partial Y_{N^l}^{(t)}}{\partial Y_{N^l-1}^{(t)}} \cdots \frac{\partial Y_l^{(t)}}{\partial w_l^{(t)}} \tag{3}$$

where η is the learning rate, N^l is the total number of hidden layers, and $Y_l^{(t)}$ is the output of hidden layer l in iteration t. The chain rule is applied here to calculate the partial derivative of parameters in each layer. Equation (1) may be used to find the partial derivative of consecutive hidden layers $\partial Y_l / \partial Y_{l-1}$.

The proposed IDCE unit consists of four CNNs, which adapt the widely-used ResNet-18 network [15] with specific loss functions for detection or classification tasks. The architecture of adapted ResNet-18 networks for Damage Classifier, Destruction Estimator, Fire Detector, and Pole Detector networks is shown in Fig. 2. In Fig. 2, input images for all CNNs are sized at $224 \times 224 \times 3$. The detailed attributes of the CNNs in the IDCE unit, including number of parameters, are summarized in Table I. The number of parameters in Destruction Estimator is considerably smaller than other networks because of removing the last 512-channel convolutional layer. This particular network has a simpler structure because it predicts only a scalar value, as explained in detail in Section II-C.

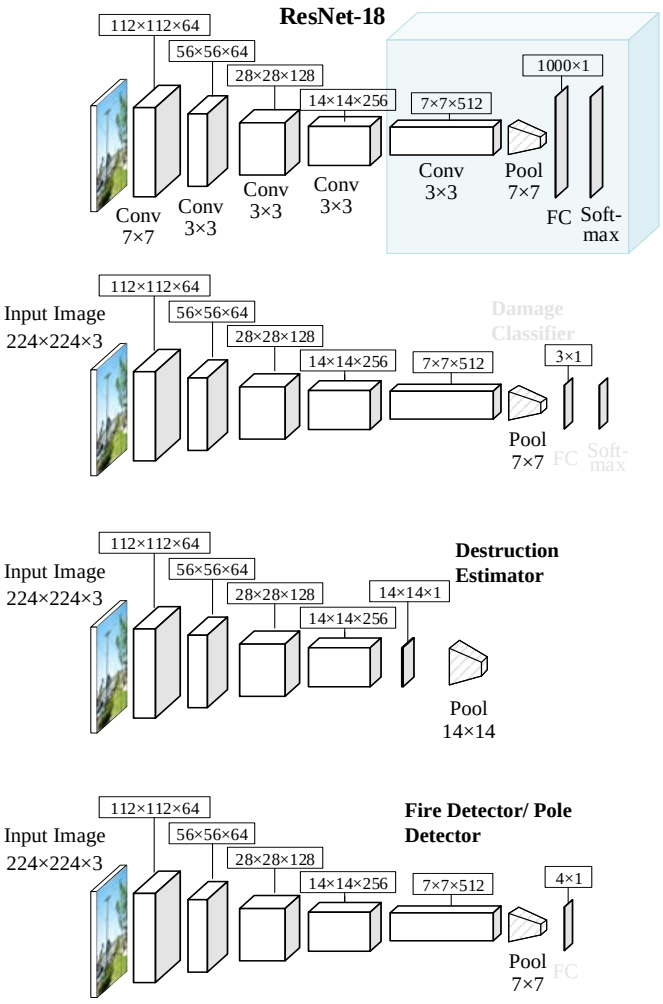

Fig. 2. Architecture of the ResNet-18 (top figure) with highlighted layers modified to make customized CNNs.

B. CNN1: Damage Detection and Classification

The distribution poles could be in different health states, which include healthy, fallen, and burning/arcing poles. In order to identify these conditions in images, we utilize a multi-class classification approach. We adopt a modified version of the ResNet-18 CNN [15], called Damage Classifier hereafter, to detect the damage type. As shown in Fig. 2, in the Damage Classifier network, the output dimension of the Fully Connected (FC) layer is updated from 1000 to 3,

This article has been accepted for publication in a future issue of this journal, but has not been fully edited. Content may change prior to final publication. Citation information: DOI 10.1109/TSG.2020.2970156, IEEE Transactions on Smart Grid

signifying the number of output classes required. The damage classifier is pre-trained using a large set of images from each class to identify the damage types. Since the training task is classification, binary cross-entropy (BCE) function is utilized as loss function. This function only rewards the correct classification for each image and is zero otherwise. It is formulated as:

$$BCE = -\sum_{i}^{N^S} \hat{\mathbf{Y}}_{1,i}.\log \mathbf{Y}_{1,i}, \tag{4}$$

where $\hat{\mathbf{Y}}_{1,i}$ and $\mathbf{Y}_{1,i}$ are one-hot encoded vectors of predicted and ground truth classifications of the i-th image in CNN1, respectively. The classification accuracy is assessed using score function s_1 defined as follows:

$$s_1 = \frac{1}{N^S}\sum_{i}^{N^S} \hat{\mathbf{Y}}_{1,i}.\mathbf{Y}_{1,i}, \tag{5}$$

which calculates the ratio of correct classifications to the total number of images.

C. CNN2: Estimation of Damage Extent in Fallen Poles

The next stage of the proposed IDCE unit is to estimate the damage extent. In this stage, the healthy poles are not assessed for damages; however, the fallen, burning and arcing ones are analyzed to estimate the damage extent, as shown in Fig. 1. If the pole is identified as fallen, another neural network, named Destruction Estimator Network, estimates how much damage the pole sustained, by producing a scalar value in $[0, 1]$, where 1 represents a 100% damage. As shown in Fig. 2, in the Destruction Estimator network the last 512-channel convolutional layer of ResNet-18 is replaced by a single channel, followed by a 14×14 average pooling layer, to produce a scalar value.

In order to standardize the damage assessment method, certain criteria are defined for qualitative damage analysis. More specifically, the percentage of damage to a fallen utility pole is defined based on the angle of tilt of the fallen electrical pole, with reference to the vertical line at 0 degrees. For instance, if the pole is tilted 30 degrees from its vertical position, the damage is assumed to be 30%. In this case, the maximum damage of 90% is estimated when the pole is fallen on the ground. In addition, if the pole is broken at some point along its height, a 30% increase is included in its damage estimation, as shown in Fig. 3, while the total damage percentage is capped by maximum of 100%. MSE

TABLE I
ATTRIBUTES OF CNNS FOR INPUT IMAGE SIZE OF $224 \times 224 \times 3$

Network Name	Output Size	Network Type	Loss Func.	Num. of Parameters
ResNet-18 [15]	1000×1	Classification	BCE	11.69 M*
Damage Classifier	3×1	Classification	BCE	11.18 M
Destruction Estimator	1×1	Regression	MSE	2.78 M
Pole Detector	4×1	Regression	MSE	11.18 M
Fire Detector	4×1	Regression	MSE	11.18 M

* million

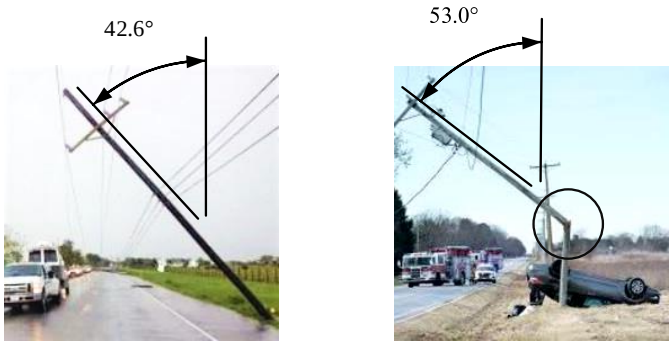

(a) (b)

Fig. 3. Damage assessment for fallen poles: a) 41.5% damage due to 41.5° tilting, b) 53% damage due to tilting plus 30% due to breaking totaling to 83% damage estimation.

loss function is used for training the network, while the results are evaluated using the mean L1 distance as scoring function, which shows the regression accuracy and is given by:

$$s_2 = \frac{1}{N^S}\sum_{i}^{N^S} |Y_{2,i} - \hat{Y}_{2,i}| \tag{6}$$

where $Y_{2,i}$ and $\hat{Y}_{2,i}$ are scalar values of the actual and predicted damage percentage for fallen pole image i in CNN2.

D. CNN3 and CNN4: Estimation of Damage Extent in Burning and Arcing Poles

If the pole is identified as burning or arcing, a bigger threat exists in the system, which must be addressed promptly. Also, estimating the extent of fire or arc in the pole is crucial to prepare for the repair operation. For that purpose, a CNN network, named Fire Detector, is trained to identify the bounding boxes of fire or arc in images of burning poles. Drawing bounding box over an object is part of object detection process, which is usually performed by CNNs. Since the photos of utility poles are not of the same scale, the area of the fire bounding boxes cannot be compared in different images and hence estimation of fire extent could be compromised. In order to resolve this issue, we train another network, called Pole Detector, to find the bounding box of the utility pole in each image, and then estimate the fire extent as the ratio of fire to the pole area.

The problem with this method is that the entire utility pole may not be captured in all images, and therefore, the identified pole area cannot be used for damage estimation. However, it is safe to assume that the widths of the poles are captured in all images. Given that we can calculate the height to width ratio of all poles in our distribution system, we can estimate the actual area of pole's bounding box based on only its width, as shown in Fig. 4. The damage extent (DE) due to fire is then formulated as:

$$DE = \frac{w_f \times h_f}{a \times w_p^2}, \tag{7}$$

where w_f, h_f are the width and height of the fire bounding box, w_p, is the width of the pole bounding box, and a is the height/width ratio of the poles.

This article has been accepted for publication in a future issue of this journal, but has not been fully edited. Content may change prior to final publication. Citation information: DOI 10.1109/TSG.2020.2970156, IEEE Transactions on Smart Grid

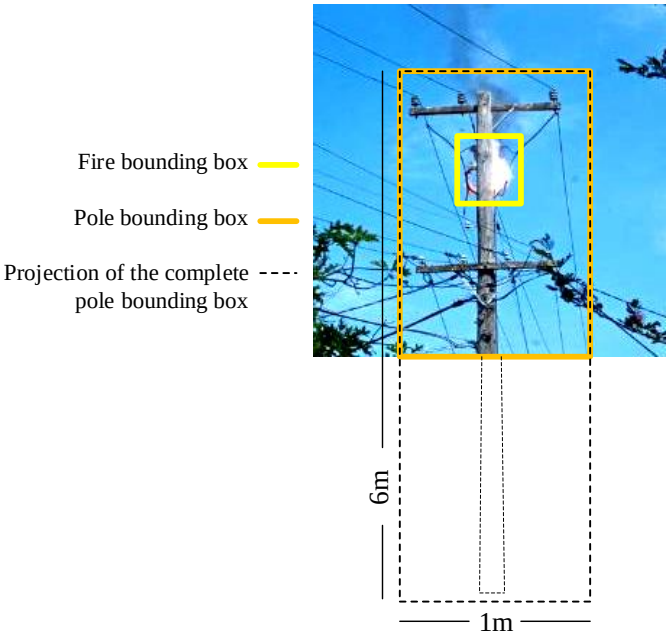

Fig. 4. Damage extent for burning poles is given by the ratio of fire bounding box area to that of complete bounding box of the pole.

The networks for Pole Detector and Fire Detector have similar structures as the Damage Classifier described previously, but without the Softmax layer at the output. This is done in order to obtain output logits, instead of output classes, for predicting the coordinates of the bounding boxes. MSE loss function is used for training Pole Detector and Fire Detector networks. The results are then evaluated using score function s_3, which measures mean L1 distance between actual and predicted bounding boxes.

$$s_3 = \frac{1}{N^S} \sum_{i}^{N^S} |\mathbf{Y}_{3,i} - \hat{\mathbf{Y}}_{3,i}|, \tag{8}$$

where $\mathbf{Y}_{3,i}$ and $\hat{\mathbf{Y}}_{3,i}$ are respectively the actual and predicted 4-dimensional output vectors of CNN3 with elements (x_i, y_i, w_i, h_i) showing the coordinates of a bounding box over pole or fire area in image i. This distance can be interpreted as average pixel deviation of predicted coordinates of a bounding box from actual values. The score function s_4 for CNN4 is defined in the same way as s_3.

III. Data Collection and Pre-Processing

There is no known existing image database towards damage estimation of this nature in utility distribution poles, hence data collection was a significant part of the effort for this paper. Online search engines were used to find relevant pole images. Then, we pre-processed the database accordingly and populated training parameters. After initial screening, 1615 images of electrical poles were selected from which 572 images are from healthy poles, 457 images from fallen ones, and 586 images from burning and arcing poles. All images must be 224×224 pixels and have 3 color channels (RGB), to be compatible with ResNet input layer. Also, before feeding the images to classification and regression networks, we apply color normalization on all of them. For color normalization, the pixel with the lowest intensity in each RGB channel is set to 0, while the highest intensity pixel is set to 255 (maximum value). Intensity of all other pixels are scaled according to each RGB channel. As visualized in Fig. 5, color normalization provides more contrast, particularly for images with dark backgrounds or the ones taken at night time.

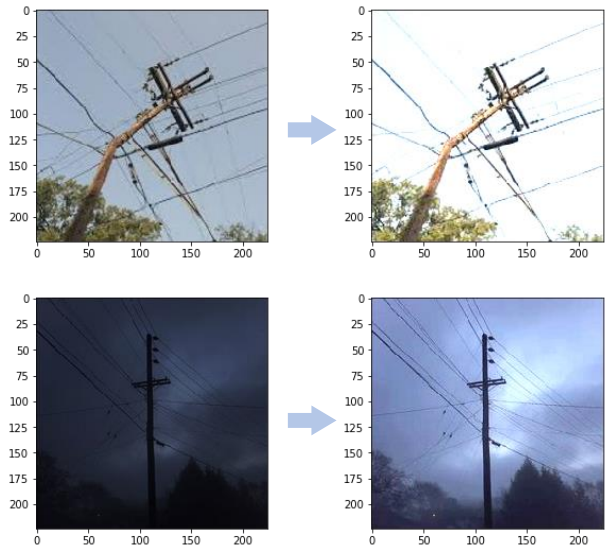

Fig. 5. Applying color normalization on input images

In order to provide a more reliable classification, three data augmentations, namely five-crop, random horizontal flipping and color jittering, are used to diversify the training set. For this purpose, all images are first resized to 300 pixels in length and, if not square, cropped evenly on both sides to be 300 pixels in width too. Then, five 224×224 crops are extracted, in which four crops are from the four corners, and one crop is from the center. Random horizontal flipping and color jittering are applied next. Using color and brightness manipulations are logically appropriate in all CNNs as images may be taken at different times of the day or different lighting conditions. Also, fire flames or arcs come in slightly different color shades in different images, therefore providing appropriate case for utilization of color jittering augmentation. For color jittering, image parameters are randomly changed at each training epoch following a normal distribution function with zero mean, and the standard deviations 0.2, 0.2, 0.2, and 0.1 respectively for brightness, contrast, saturation, and hue.

IV. Numerical Study

A. Training and Validation of the Neural Networks

The four CNNs of the IDCE are trained independently with relevant train data sets. For each training, the whole data set is divided into $[0.6, 0.2, 0.2]$ parts for training, validation, and testing, respectively, where the validation set is used for tuning the hyper parameters, such as learning rate or batch size, through cross-validation. In cross-validation method, the whole training and validation parts are divided into k folds (4 in this case) and in each round, one fold is taken as

This article has been accepted for publication in a future issue of this journal, but has not been fully edited. Content may change prior to final publication. Citation information: DOI 10.1109/TSG.2020.2970156, IEEE Transactions on Smart Grid

validation and $k-1$ folds as training set. Then for each hyper-parameter, the network is trained over a range of values using only the training set, and the results are evaluated using the validation set. The hyper-parameter with the best result through all validation folds is selected as the final training parameter. Training parameters and validation results for each network are presented next.

1) Damage Classifier (CNN1): Input data set for damage classifier network includes images from all classes, while output includes classification of pole state into one of three classes. For training the network, Adam algorithm [28] is used as the optimizer with learning rate of 2×10^{-5}, and first and second order momentums set to 0.9 and 0.999, respectively. Input data set is trained for 30 epochs with batch size of 64.

The results show that after 30 epochs, the model can reach to 96.16% accuracy on the validation set. This value is 94.54% on the test data set, which indicates robustness of the network to unseen data. Fig. 6 shows variation of score function s_1 (5) and BCE loss function as the model is being trained with Adam optimizer. The validation accuracy of classification in different classes is shown in Fig. 7. In Fig. 7, classification accuracy is over 94% for all classes, where burning and fallen poles are classified better than healthy poles. That is partly because in images of healthy poles, there might be other fallen objects and possible light glare that make the model classify them into fallen or burning classes respectively.

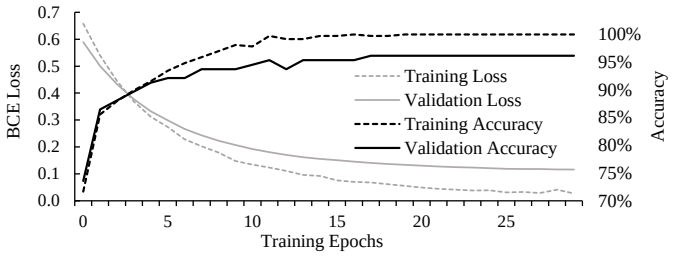

Fig. 6. Variation of BCE loss and score functions during training of the damage classifier network

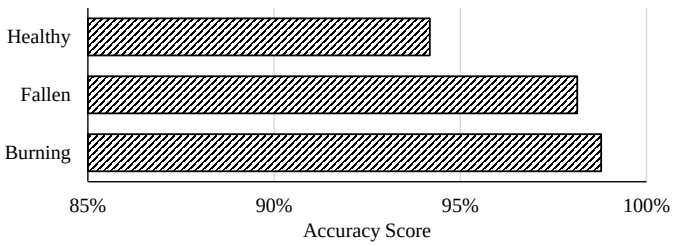

Fig. 7. Classification accuracy of the damage classifier for different classes

2) Destruction Estimator (CNN2): Input training data set for CNN2 includes only images of fallen poles. The output is a scalar value predicting damage extent of fallen poles, as quantified in Section II. The Adam optimizer with the same parameters as the one for CNN1 is chosen for training, except with the learning rate set to 2×10^{-5}. We also used batch size 32 and 100 training epochs. The variations of MSE loss function during training is shown in Fig. 8, which reaches

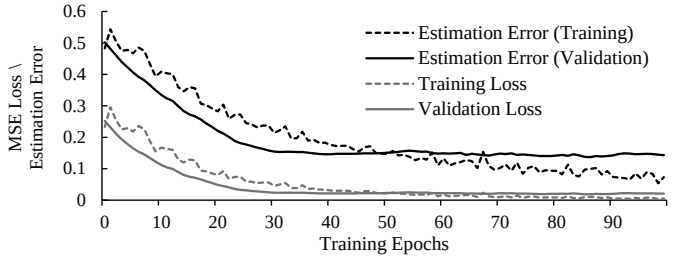

Fig. 8. MSE loss and estimation error during training of the Destruction Estimator Network

to 0.0204 at the end. Variation of score function (6) is also shown in the same figure, which shows final estimation error of 0.1429 on validation set. Since the range of normalized values being predicted is in $[0, 1]$, loss value of 0.1429 means that the destruction estimator can predict the damage for fallen poles with 14.29% error. Further, the estimation error on the test data is 15.43%. A part of this error may be associated with the simplified method used here for labeling fallen images.

3) Pole Detector and Fire Detector (CNN3 and CNN4): CNN3 and CNN4 employ the same structure as each other for the purpose of estimating. Input training data set for the Pole Detector includes all images, while the Fire Detector takes only burning and arcing images as input. The actual bounding box of the pole and the damage percentage due to fire or arc is estimated by applying the known aspect ratio of the poles as in (7). In this work, we assume all utility poles have a height/width ratio of 6. For training, Adam optimizer is used with the same momentums as CNN1, and learning rate of 0.001. We also used batch size 64 and 200 epochs for training.

The decreasing trend of the score function during the training of Pole Detector is shown in Fig. 9. The final average deviation in the Pole Detector, which predicts bounding boxes of poles, is 20.39 pixels on the validation set. In essence, each coordinate of the bounding boxes is predicted with about 20 pixels error over a 224×224 image. This deviation on test data sets is 21.32 pixels. The Fire Detector, with the same structure as the one for Pole Detector, finds it more difficult to predict the coordinates of fire and can only converge to the average deviation of 23.39 pixels on the validation set. This difference can be explained by the more complicated shape of fire flame and arc compared to pole structure. Furthermore, in some burning or arcing images, particularly the ones taken over darker background, there is a camera flare that makes it harder to define solid bounding boxes over fire/arc.

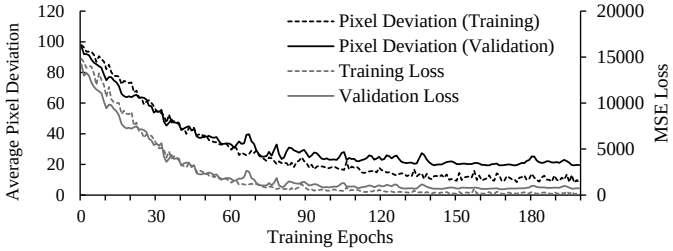

Fig. 9. Variation of MSE loss function and average estimation error of coordinates of pole bounding box (in pixels) during training of Pole Detector

This article has been accepted for publication in a future issue of this journal, but has not been fully edited. Content may change prior to final publication. Citation information: DOI 10.1109/TSG.2020.2970156, IEEE Transactions on Smart Grid

B. Testing the Neural Networks

Testing data set consists of 20% of all images that remain unseen to trained networks during training or validation. Test images are fed into the IDCE to predict the pole state and estimate the damage extent if damages are present in the image. Applying test images to the damage classifier results in classification accuracy of 94.54%, which is very close to the validation score of 96.16%. Images classified as fallen by the CNN1 (damage classifier), regardless of classification correctness, are fed to the Destruction Estimator CNN2 to estimate the damage extent. For images classified as fallen in error, the ground truth is set to 0. The obtained estimation error is 19.01% on input images. This is higher than 14.29% error on the validation set and the main contributors to that are the images classified as fallen by mistake.

All test images are fed to the Pole Detector to find the bounding box of the pole area. Applying this network to the test images results in estimation error of 21.56 pixels, which is close to 20.39 pixel deviation on the validation set. Figure 10 shows four of the predicted bounding boxes of poles versus ground truth. In Fig. 10, the predicted bounding boxes have enough ability to identify the main and largest pole in the picture. However, in the lower right image in Fig. 10, it is shown that finding a proper bounding box over broken or deformed poles are more challenging.

Test images classified as burning/arcing by the damage classifier are fed to Fire Detector to find the bounding boxes of fire/arc area. Applying this network to the test input images results in estimation error of 23.11 pixels. The predicted bounding boxes of fire/arc versus ground truth for four test images are shown in Fig. 11. A noteworthy observation in the images in Fig. 10 and 11 is that even though the predicted bounding boxes are not always perfectly aligned with the ground truth, their areas are very close in most samples. It is partly because of the fact that the bounding boxes are defined by a starting point coordination (x, y) and the width and height of the box (w, h). If only width and height are estimated with a low error, the box area is obtained with a good approximation. This result helps us identify the damage extent, as it is defined by the area of fire over bounding boxes in (7).

In the final stage of testing the IDCE unit, the outputs from Pole Detector and Fire Detector are utilized to estimate the damage extent due to fire/arc, using the method in Section II. The average damage estimation error on the test data set of burning/arcing images is calculated as 9.61%. In Fig. 12, the predicted damage extent due to fire, calculated by (7), is compared with the ground truth for a number of test samples, where the estimation error for small damages is less than the error for larger ones. One reason for this is that in images showing huge fire flames, parts of the fire may fade into the background, and become harder to detect by the model.

The training and prediction times, along with number of training samples and epochs are shown in Table II for all CNNs. The training samples in this table include both training and validation sets, because both of them contribute to the training time. In general, the regression-based CNNs (for Pole and Fire Detector) takes more time to train than the classifier network. However, the Damage classifier takes the most per epoch training time because of the larger number of training samples. The shortest training time per epoch is for Destruction Estimator because of its smaller number of training samples, and also less parameters in its structure. The prediction time, is similar for all networks and all of them can predict their desire output in around 6 milliseconds which is almost real-time.

As discussed earlier in this section, the classification scores in healthy images are lower than the other two. Table III shows

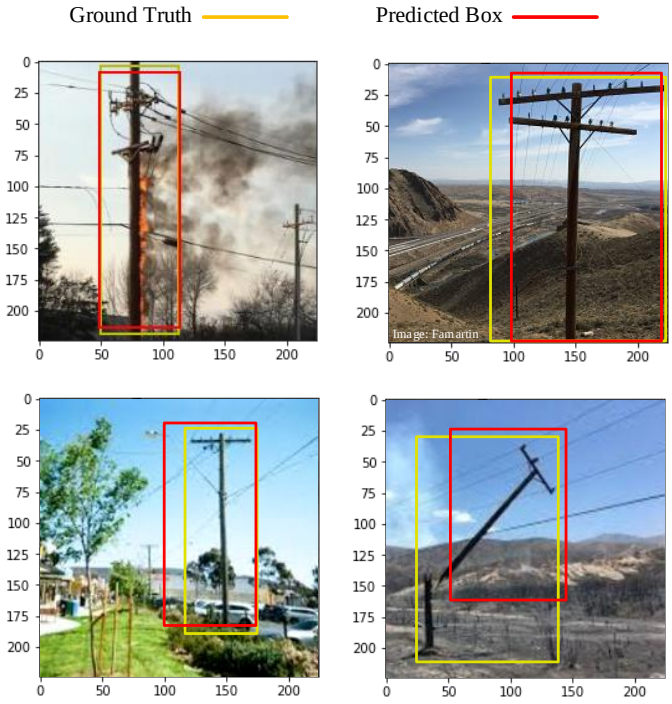

Fig. 10. Predicted pole bounding boxes over four test images.

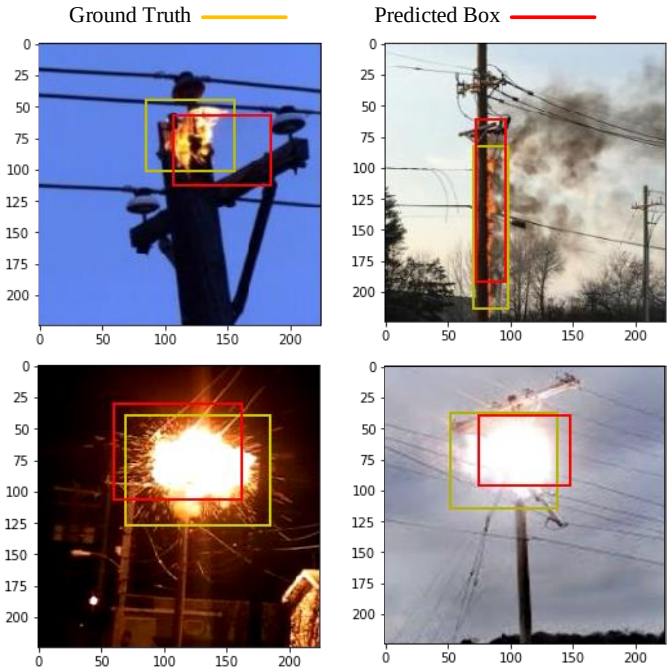

Fig. 11. Predicted fire/arc bounding boxes over four test images.

This article has been accepted for publication in a future issue of this journal, but has not been fully edited. Content may change prior to final publication. Citation information: DOI 10.1109/TSG.2020.2970156, IEEE Transactions on Smart Grid

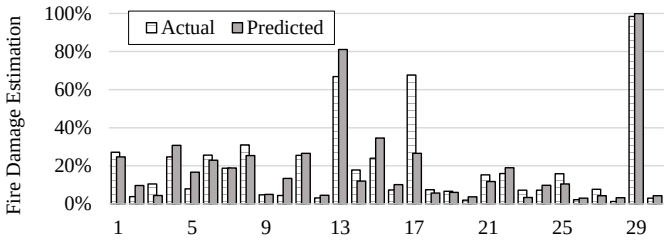

Fig. 12. Fire/arc damage estimation accuracy for a number of burning test samples

TABLE II
TRAINING AND PREDICTION TIMES OF THE NETWORKS

Network	Train samples	Train epochs	Train time (sec)	Pred. time (sec/image)
Damage Classifier	1292	30	204.6	0.006
Destruction Estimator	366	100	138.9	0.005
Pole Detector	469	200	402.0	0.006
Fire Detector	469	200	392.4	0.006

where these wrong classifications took place. Even though the overall classification error is low (below 4%), most existing errors happen when healthy images are mistakenly classified as fallen and burning. The amount of fallen images classified as healthy is also relatively high. This is mainly because of the fact that the fallen poles are classified by identifying tilted or broken lines in the image. Therefore, any fallen or tilted object in the image might confuse the model. On the other hand, the unique shape of fire and arc results in less mistakes in classification of burning poles, which is close to 99%.

TABLE III
CLASSIFICATION CONFUSION MATRIX OVER TEST IMAGES

		Predicted classes: Healthy	Fallen	Burning
Actual class	**Healthy**	94.18%	3.49%	2.33%
	Fallen	2.29%	97.14%	0.57%
	Burning	0.55%	0.67%	98.78%

C. Sample Application in Distribution Network Restoration

UAVs can be utilized to fly over distribution lines and take images and record the geographical location of distribution poles. The pole location and images can be then utilized by the proposed IDCE unit to identify and display pole damages on utility outage management systems. This application would help the system operators to make informed decisions for immediate responding, as well as manage limited repair resources after widespread events. Given the low operational cost of UAVs, they may fly repeatedly over distribution lines and record the development of damage over time, or observe the progress made during repair operation.

A sample application of the IDCE unit for distribution system restoration is shown in Fig. 13, where the hypothetical

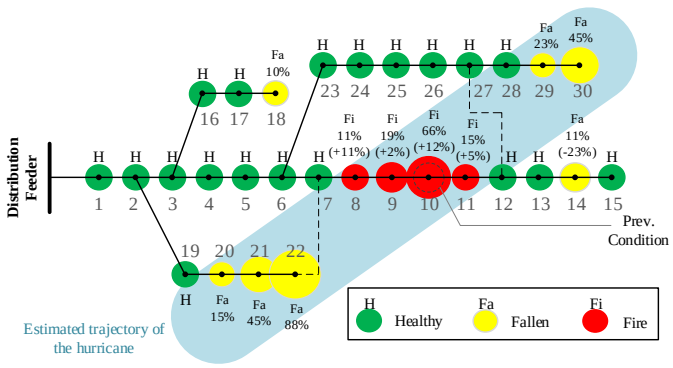

Fig. 13. Visualizing the results of IDCE analysis for damage classification and estimation on a test distribution system. The IDCE analysis helps estimating the trajectory of hurricanes, as well as trends of damage development.

results of IDCE analysis following a hurricane on a test distribution system is visualized. Such information show that the hurricane moved along a line drawn from the top right of the figure to bottom left, causing fire and pushing down some poles on its way. Further, repeated inspections by a UAV over the distribution network has recorded increase or decrease of damages on poles 8-11. Such an image indicates that the extent of damage due to fire is increasing in these poles, and they should be put on higher repair priority for extinguishing fire and repairing the poles. Using the geographical distribution of the damages in Fig. 13, the service may be restored to poles 12 and 13 via tie-switch between 12 and 27, providing that they are isolated from fire and arc areas (see e.g., [29], [30] for more details on restoration operation of distribution systems). This information is particularly valuable, because some physical damages or even fire does not cause an immediate outage of the pole, and hence the electrical signals received from local protection devices may not be fully reliable.

V. CONCLUSION

This work contributes to utility restoration processes following the occurrence of a disruptive event by providing an automated damage classification and quantification framework. The proposed architecture, consisting of four CNNs, can efficiently capture nuances in images of different resolutions, scales and background and promises to reduce inspection and damage detection time. The ResNet architecture is used as a base for the CNNs, both for classification and regression purposes, creating a series of networks capable of classifying the damage and estimating its extent on each pole. The proposed model estimates the damage extent in fallen poles based on their apparent tilting or breaking, while in burning and arcing poles the damage is estimated by the ratio of the areas of fire to pole bounding boxes. Although high accuracy is achieved in the classification of healthy and fallen poles, burning and arcing poles proved harder to detect. The specific topic of training networks to detect fire in poles has a particular application in power systems and may be of interest in future research. In particular, image processing methods and larger training image dataset may contribute to higher accuracy of detecting burning poles.

REFERENCES

[1] S. Folga, M. McLamore, L. Talaber, and A. Tompkins, "National electricity emergency response capabilities," Department of Energy, Office of Energy Policy and Systems Analysis, Tech. Rep., 2016.

[2] J. Muhs and M. Parvania, "Stochastic spatio-temporal hurricane impact analysis for power grid resilience studies," in *2019 IEEE Power & Energy Society Innovative Smart Grid Technologies Conference (ISGT)*, 2019, pp. 1–5.

[3] C. Zamuda, B. Mignone, D. Bilello, K. Hallett, C. Lee, J. Macknick, R. Newmark, and D. Steinberg, "Us energy sector vulnerabilities to climate change and extreme weather," Department of Energy Washington DC, Tech. Rep., 2013.

[4] "Power outage annual report: Blackout tracker," Eaton, Tech. Rep., 2017.

[5] V. N. Nguyen, R. Jenssen, and D. Roverso, "Intelligent monitoring and inspection of power line components powered by uavs and deep learning," *IEEE Power and Energy Technology Systems Journal*, vol. 6, no. 1, pp. 11–21, 2019.

[6] J. Toth, N. Pouliot, and S. Montambault, "Field experiences using linescout technology on large bc transmission crossings," in *2010 1st International Conference on Applied Robotics for the Power Industry*. IEEE, 2010, pp. 1–6.

[7] L. Matikainen, M. Lehtomäki, E. Ahokas, J. Hyyppä, M. Karjalainen, A. Jaakkola, A. Kukko, and T. Heinonen, "Remote sensing methods for power line corridor surveys," *ISPRS Journal of Photogrammetry and Remote Sensing*, vol. 119, pp. 10–31, 2016.

[8] "Power outage annual report: Blackout tracker," Eaton, Tech. Rep., 2015.

[9] L. Arreola, A. M. de Oca, A. Flores, J. Sanchez, and G. Flores, "Improvement in the uav position estimation with low-cost gps, ins and vision-based system: Application to a quadrotor uav," in *2018 International Conference on Unmanned Aircraft Systems (ICUAS)*. IEEE, 2018, pp. 1248–1254.

[10] J. Toth and A. Gilpin-Jackson, "Smart view for a smart grid—unmanned aerial vehicles for transmission lines," in *2010 1st International Conference on Applied Robotics for the Power Industry*. IEEE, 2010, pp. 1–6.

[11] S. Ren, K. He, R. Girshick, and J. Sun, "Faster r-cnn: Towards real-time object detection with region proposal networks," in *Advances in neural information processing systems*, 2015, pp. 91–99.

[12] J. Redmon, S. Divvala, R. Girshick, and A. Farhadi, "You only look once: Unified, real-time object detection," in *Proceedings of the IEEE conference on computer vision and pattern recognition*, 2016, pp. 779–788.

[13] W. Liu, D. Anguelov, D. Erhan, C. Szegedy, S. Reed, C.-Y. Fu, and A. C. Berg, "Ssd: Single shot multibox detector," in *European conference on computer vision*. Springer, 2016, pp. 21–37.

[14] K. Simonyan and A. Zisserman, "Very deep convolutional networks for large-scale image recognition," *arXiv preprint arXiv:1409.1556*, 2014.

[15] K. He, X. Zhang, S. Ren, and J. Sun, "Deep residual learning for image recognition," in *Proceedings of the IEEE conference on computer vision and pattern recognition*, 2016, pp. 770–778.

[16] C. Szegedy, S. Ioffe, V. Vanhoucke, and A. A. Alemi, "Inception-v4, inception-resnet and the impact of residual connections on learning," in *Thirty-First AAAI Conference on Artificial Intelligence*, 2017.

[17] J. Deng, W. Dong, R. Socher, L.-J. Li, K. Li, and L. Fei-Fei, "Imagenet: A large-scale hierarchical image database," in *2009 IEEE conference on computer vision and pattern recognition*. Ieee, 2009, pp. 248–255.

[18] Z. Hu, T. He, Y. Zeng, X. Luo, J. Wang, S. Huang, J. Liang, Q. Sun, H. Xu, and B. Lin, "Fast image recognition of transmission tower based on big data," *Protection and Control of Modern Power Systems*, vol. 3, no. 1, p. 15, 2018.

[19] B. Chen and X. Miao, "Distribution line pole detection and counting based on yolo using uav inspection line video," *Journal of Electrical Engineering & Technology*, pp. 1–8, 2019.

[20] C. Martinez, C. Sampedro, A. Chauhan, and P. Campoy, "Towards autonomous detection and tracking of electric towers for aerial power line inspection," in *2014 International Conference on Unmanned Aircraft Systems (ICUAS)*. IEEE, 2014, pp. 284–295.

[21] B. Song and X. Li, "Power line detection from optical images," *Neurocomputing*, vol. 129, pp. 350–361, 2014.

[22] L. Zhu, W. Cao, J. Han, and Y. Du, "A double-side filter based power line recognition method for uav vision system," in *2013 IEEE International Conference on Robotics and Biomimetics (ROBIO)*. IEEE, 2013, pp. 2655–2660.

[23] O. Menéndez, M. Pérez, and F. Auat Cheein, "Visual-based positioning of aerial maintenance platforms on overhead transmission lines," *Applied Sciences*, vol. 9, no. 1, p. 165, 2019.

[24] J. Lu, Y. Ye, X. Xu, and Q. Li, "Application research of convolution neural network in image classification of icing monitoring in power grid," *EURASIP Journal on Image and Video Processing*, vol. 2019, no. 1, p. 49, 2019.

[25] Y.-p. Zhong, Q. Zuo, Y. Zhou, and C. Zhang, "A new image-based algorithm for icing detection and icing thickness estimation for transmission lines," in *2013 IEEE International Conference on Multimedia and Expo Workshops (ICMEW)*. IEEE, 2013, pp. 1–6.

[26] J. Ahmad, A. S. Malik, L. Xia, and N. Ashikin, "Vegetation encroachment monitoring for transmission lines right-of-ways: A survey," *Electric Power Systems Research*, vol. 95, pp. 339–352, 2013.

[27] "Signal search: Cellphone service after major hurricanes," https://www.wsj.com/articles/signal-search-cellphone-service-after-major-hurricanes-1539877736, accessed: 2019-11-20.

[28] D. P. Kingma and J. Ba, "Adam: A method for stochastic optimization," *arXiv preprint arXiv:1412.6980*, 2014.

[29] M. M. Hosseini, A. Umunnakwe, and M. Parvania, "Automated switching operation for resilience enhancement of distribution systems," in *2019 IEEE Power & Energy Society General Meeting*, 2019, pp. 1–5.

[30] H. T. Nguyen, J. Muhs, and M. Parvania, "Assessing impacts of energy storage on resilience of distribution systems against hurricanes," *Journal of Modern Power Systems and Clean Energy*, vol. 7, no. 4, pp. 731–740, 2019.